Supplemental Materials
Supplemental Figures

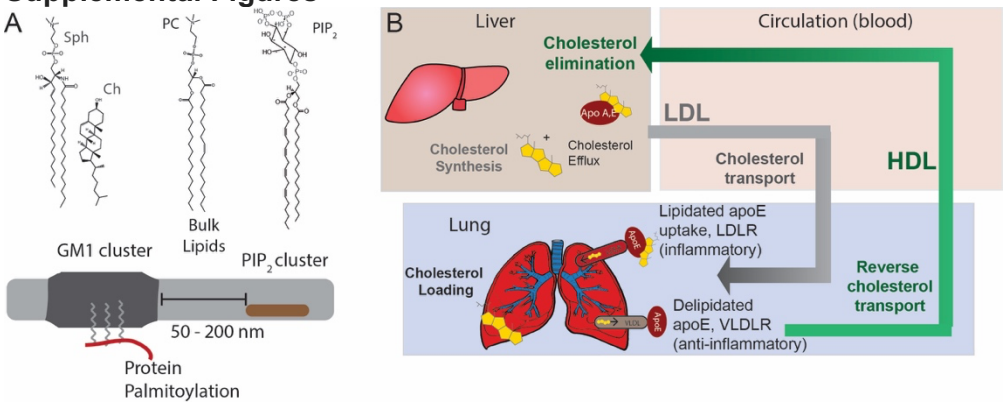

Figure S1. Cholesterol transport and function in GM1 clusters (**A**) The side view of a plasma membrane is shown (top extracellular). The membrane partitions into regions of ordered (saturated) and disordered (unsaturated) lipids. The ordered region contains cholesterol and sphingolipids (Sph). Packing of cholesterol with saturated lipids is thought to provide order and makes ordered lipids thicker than disordered lipids. The disordered region contains unsaturated lipids including phosphatidylcholine (PC), phosphatidic acid (PA), and phosphatidylinositol 4,5-bisphosphate (PIP_2). PIP_2 and PA are signaling lipids and PIP_2 forms its own lipid domains separate from GM1 clusters. Palmitoylation of proteins typically occurs on the cytosolic portion of the membrane and inserts into the inner leaflet (red line with lipids attached). For a virus that exits the cell the palmitoylation may insert into the extracellular leaflet. (**B**) Cartoon of cholesterol loading into lung pneumocyte's and macrophages. In healthy individuals most *de novo* synthesis of cholesterol takes place in the liver. Cholesterol effluxes through ATP binding cassette (ABC) transporters (not shown) and is loaded into apolipoproteins (e.g., A and E; apoA and apoE). The cholesterol is then transported through the blood serum in the form of high- and low- density lipoproteins to the lung. In the lung, low density lipoprotein receptors (LDLR) located on individual cell membranes (shown as one receptor for simplicity) take up lipidated apoE. In healthy individuals, delipidated apoE binds to the very low density lipoprotein receptor (VLDLR) and export excess cholesterol from the plasma membrane where it is transported back to the liver for elimination. During chronic inflammation reverse cholesterol transport is inhibited and cholesterol is loaded into macrophage rich tissues in the periphery.

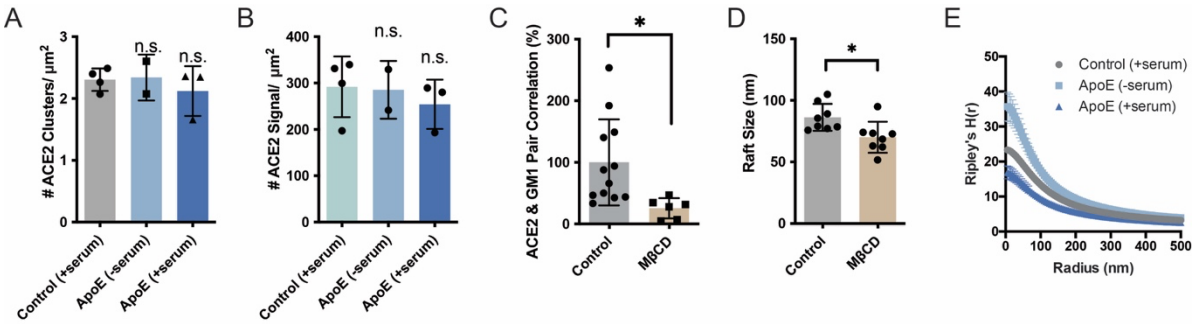

Figure S2. dSTORM of ACE2. (**A-B**) ACE2 cluster density(A) and ACE2 signal density(B) shows that the expression of ACE2 remains roughly constant when cells are loaded or unloaded with cholesterol by the cholesterol transport protein apoE. Although, while not statistically significant ACE2 expression appears to slightly decrease in high cholesterol (apoE + serum) which agrees with the clinical findings of decreased ACE2 surface expression in older people. Data are expressed as mean ± SD, n.s. P>=0.05, one-way ANOVA. (**C**) Cholesterol depletion with methyl-beta-cyclodextrin (MβCD) diminishes ACE2's cluster localization. (**D**) Cholesterol depletion by MβCD robustly decreases the apparent size of GM1 clusters after CTxB clustering. Data are expressed as mean ±SD, *P<0.05, two-sided Student's t-test. (**E**) Ripley's H-Function (H(r)) showing cluster separation after cholesterol depletion while distance between clusters gets shorter as apoE transports cholesterol from serum into the membrane.

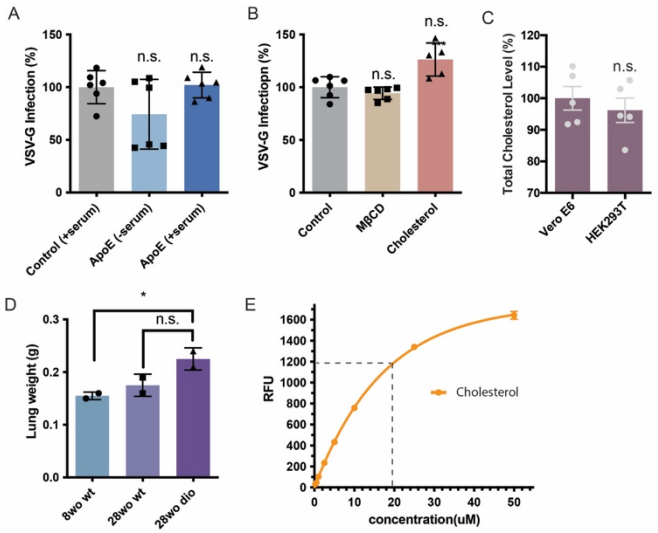

Figure S3. ACE2 over expression and VSV-G viral entry. (**A-B**) Cells were treated with apoE/MβCD and a luciferase expressing retrovirus pseudotyped with the VSV-G protein. VSV-G is a similar but distant virus compared to SARS-CoV-2 and serves as a control for age-dependent cholesterol selectivity. Infectivity was monitored by a luciferase activity in cells treated with apoE or MβCD to modulate membrane cholesterol level. (**C**) Comparison of total cholesterol in cultured VeroE6 and HEK293T cells. Free cholesterol is in the plasma membrane and cholesteryl ester is in the internal store. (**D**) Lung weight per mg of lung tissue. Lungs were extracted from 8-week-old (wo) and 28wo mice, fixed and assayed for cholesterol with a fluorescent assay. Data are expressed as mean ± SD, n.s.>0.05, one-way ANOVA. (**E**) Standard curve for lung cholesterol assay. Cholesterol in DMSO was added dose dependently and assayed for cholesterol. A wt. control lung was sectioned ~ 2-3 mg pieces homogenized and assayed for cholesterol. Dotted grey line shows how concentration of cholesterol was determined for a given RFU.

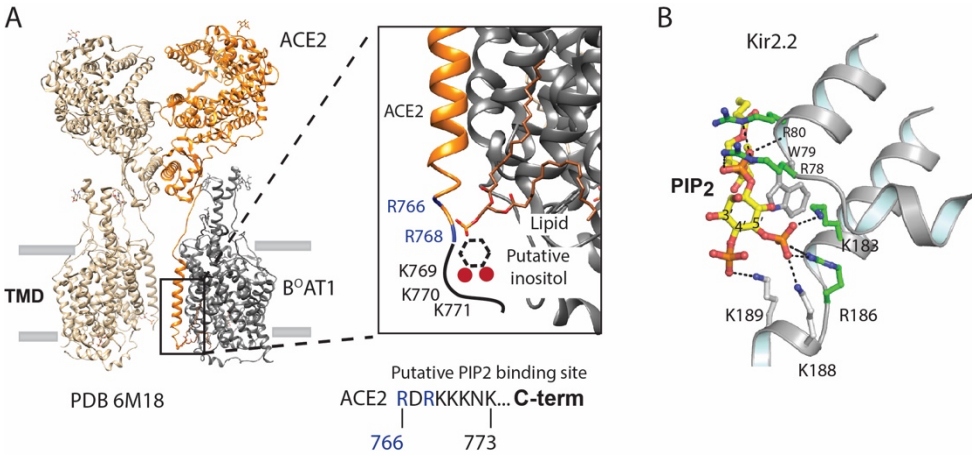

Figure S4 Anionic lipid binding site in ACE2. (**A**) The cryoEM structure of ACE2 (orange shading) in complex with B^0AT1 (Grey) (PDB 6M18) (65). A zoom of an anionic lipid binding site in the C-terminus of ACE2 is shown. The lipid presumably copurifies with the complex. Arginine residues 766 and 768 are visible in the structure (shown in blue) and adjacent to the anionic lipid. An additional 4 lysine residues are not visible in the structure but immediate follow Arg768. Presumably, PIP_2 binding occurs at this anionic lipid site. A hypothetic cartoon of inositol and two phosphates is shown as a hexagon and red dots positioned with the lysines. The acyl chains of the anionic lipid bind primarily to B^0AT1 in the complex. (**B**) For comparison, PIP_2 is shown bound to the inward rectifier potassium channel 2.2 (Kir2.2). Lysine residues extending from the transmembrane helix coordinate the two phosphates on the inositol ring. Adapted from (67) with permission under the creative license (CC BY-NC-ND 4.0).